RSC Sustainability

ROYAL SOCIETY OF CHEMISTRY

COMMUNICATION

View Article Online
View Journal | View Issue

Open Access Article. Published on 27 March 2024. Downloaded on 12/4/2025 5:26:13 PM.
This article is licensed under a Creative Commons Attribution-NonCommercial 3.0 Unported Licence.

Check for updates

Cite this: *RSC Sustainability*, 2024, **2**, 1363

Received 20th January 2024
Accepted 11th March 2024

DOI: 10.1039/d4su00026a

rsc.li/rscsus

Phosphate-based phosphor for the urban mining of lanthanides: a case study of samarium†

Yonglin Chen, Haoyi Wu * and Yihua Hu *

The recycling of samarium ions (Sm^{3+}) from the crystalline $NaBaPO_4$-based phosphor to an optical glass was realized in a green and sustainable way. The solubility of $NaBaPO_4$:Sm^{3+} luminescent material enables its complete dissolution in water with a small amount of phosphoric acid. By adjusting the pH to alkaline values, a precipitate was obtained. This precipitate was annealed with additional Na_2CO_3 and $NH_4H_2PO_4$ and a transparent glass with orange-red fluorescence was obtained, indicating that Sm^{3+} was successfully recycled from the phosphor to the glass. The recovery efficiency of Sm^{3+} ions reaches 97.6%. Thus, a facile method to recycle a type of lanthanide from a phosphate-based phosphor for urban mining is reported in this work.

Sustainability spotlight

In this study, the recycling process of Sm^{3+} from a phosphate-based phosphor to an optical glass was introduced. In this process, the Sm^{3+} ions could be obtained with the dissolution of the $NaBaPO_4$ phosphor. These Sm^{3+} ions could be used in the preparation of optical glass. Then, an example for urban mining of lanthanides in a green and sustainable way was demonstrated with the use of phosphoric acid, which was used to assist the dissolution of the phosphor.

Rare earth elements, often known as industrial vitamins, are a fundamental driver of industrial revolution 4.0. The 4f electronic state transitions (*i.e.* 4f–4f and 5d–4f) of lanthanides enable them to have wide applications in optics, catalysis, magnetics and so forth.[1–4] Unfortunately, lanthanides are non-renewable resources. In China, the reserves of rare earth elements, whose majority are the lanthanides, decreased from 55 million tons to 44 million tons from 2013 to 2020 due to the fast consumption speed of the industry. This decreased reserve indicates the shortcoming of lanthanide consumption only from natural mineral mining. Urban mining of lanthanides, in which the elements are recycled from urban wastes, is one of the possible methods to ensure the sustainable usage of lanthanides.[5,6]

Thousands of tons of lanthanide elements are consumed in the lighting industry annually as phosphors use lanthanides to convert light to various colors.[7–12] In the process of rapid urban development, waste phosphors are inevitably produced, and the recovery of valuable rare earth elements from industrial residues and by-products is a very challenging issue to achieve zero waste production in the circular economy. Thus, for economic and circular benefits, rare earth ions need to be recycled.[7]

Most commercial phosphors are synthesized with alumina or silicate hosts since they are physically and chemically stable. It is difficult to extract lanthanides from these hosts unless dangerous strong acids such as hydrochloric acid and sulphuric acid are employed to corrode them.[13–15] The use of strong acids is usually restricted in many industrial cases because of their strong corrosiveness and toxicity. As compared to their alumina- and silicate-based counterparts, phosphate-based phosphors have excellent luminescent properties but have a relative hydrolytic tendency.[16,17] Thus, phosphate-based phosphors are soluble to a certain degree, making the sustainable metallurgy of lanthanides possible. Phosphor-based phosphor recovery and utilization of secondary rare earth resources to achieve a sustainable circular economy are important options to meet future raw material needs.

Herein, the extraction of samarium (Sm^{3+}), which is one of the lanthanides with orange-red emission and used in warm light emitting diodes (wLEDs), was achieved in an $NaBaPO_4$ (denoted as NBP) orthophosphate structure. The Sm^{3+}-doped $NaBaPO_4$ (denoted as NBPS) was found to be partially soluble in water. By adding a small amount of phosphoric acid, the sample dissolved completely at a pH of about 2–3. The Sm^{3+} was separated from the solution using extraction and precipitation. Accompanied by co-precipitated Ba^{2+} compound, sodium carbonate and ammonium biphosphate, a glass with orange-red emission was successfully synthesized using a high-

Sachool of Physics and Optoelectronic Engineering, Guangdong University of Technology, Wai Huan Xi Road, No. 100, Guangzhou 510006, China. E-mail: manofchina@outlook.com; why@gdut.edu.cn; huyh@gdut.edu.cn

† Electronic supplementary information (ESI) available. See DOI: https://doi.org/10.1039/d4su00026a

Open Access Article. Published on 27 March 2024. Downloaded on 12/4/2025 5:26:13 PM.
This article is licensed under a Creative Commons Attribution-NonCommercial 3.0 Unported Licence.

temperature treatment. The recycling process of Sm^{3+} from phosphor and its reusability in the subsequent materials synthesis were demonstrated. Moreover, the use of phosphoric acid was safer rather than the strong acids. Surprisingly, this type of phosphor does not require any pretreatment and can be leached directly with phosphoric acid. Therefore, the urban mining of lanthanides from waste lighting devices was shown to be possible.

The recycling of Sm^{3+} is depicted in Fig. 1. The Sm^{3+} ion (5 mol%)-doped NBP in 1.0 g is dispersed in distilled water. Part of the sample was dissolved and the redundant part (about 0.97 g) was dispersed in water homogeneously (Fig. 1c). A strong scattering of the red laser conformed the cloudy solution. The dissolution of the dispersion needed a large amount of water (Fig. S1†) until a small amount of phosphoric acid was added to adjust the pH to 2–3. Then, the sample dissolved completely to give a transparent solution A (Fig. 1d). According to ICP-MS, the concentration of Sm^{3+} was about 4.172 mg L^{-1} in the solution (Table S2†). Thus, the solution contained about 0.016 mmol Sm^{3+} ions (5.0 mol% in 1.0 g NBP).

Two conclusions could be drawn. First, all the Sm^{3+} ions were dissolved in the solution with a proper amount of phosphoric acid, and they were detectable using ICP-MS. Second, the Sm^{3+} ions could be separated from the solution using extraction and precipitation, indicating that the ions were recyclable from the NBP host.

For the NBP host, Ba^{2+} and Sm^{3+} were co-precipitated in solution A. During this process, 0.1 M NaOH solution was added into solution A to adjust the pH to 9. Afterward, a white precipitate containing Ba^{2+} and Sm^{3+} compounds was observed. The precipitate was centrifuged and dried to obtain a white powder (Fig. 1e). The concentration of Sm^{3+} in the residual solution was analysed with ICP-MS. The result indicated that only about 2.4% of the total Sm^{3+} ions remained in the residual solution and 97.6% of the Sm^{3+} was precipitated (Table S2†), together with the Ba^{2+} ions. For comparison, in Table 1, the results reported in the literature concerning the lanthanides recovery are listed. As compared, the high recovery rate is reached in the present work.

The XRD analysis of the precipitate indicated the presence of $BaHPO_4$ (Fig. S2†), and Sm^{3+} was precipitated in the form of $Sm(OH)_3$ (Fig. S3†), but fluorescence was not notable in the compound. This precipitate could be reused to produce NBPS or other materials.

An optical glass was produced as a prototype to demonstrate the reusability of the recovered Sm^{3+} ions. The glass showed a red-orange emission under UV excitation (Fig. 1f). The emission colour was similar to that of NBPS, indicating that Sm^{3+} was successfully incorporated into the glass (the sample was denoted as GS). Therefore, the XRD patterns and emission spectra confirmed that Sm^{3+} ions precipitated in the form of $Sm(OH)_3$ when the pH is adjusted to alkalinity. In this case, the recycling of Sm^{3+} is successful (Fig. S3†).

The structures of the NBPS and GS were determined with X-ray diffraction (XRD). As shown in Fig. 2a, according to the Joint Committee on Powder Diffraction Standards, the XRD patterns recorded for NBPS were identically matched to the JCPDS No. 81-2250,[21] indicating an orthorhombic crystalline structure. According to the Scherrer formula, the characteristic crystalline size of the sample was about 5.36 nm, indicating a considerable crystallization in the structure. The structure of NBPS is constructed by Na–O and Ba–O–P layers. The Sm^{3+} ions occupied the Na^{+} sites when they were doped into the lattice because of

Table 1 Lanthanide ion recovery levels reached in the literature

Materials	Recovery rate of rare earth elements	Ref.
NBP:Sm^{3+}	97.6%	This work
Coal fly ash	89%	6
NdFeB slurry	1.09%	18
RE/$CaSO_4$	97%	19
$SrAl_2O_4$:Eu^{3+}	83%	20

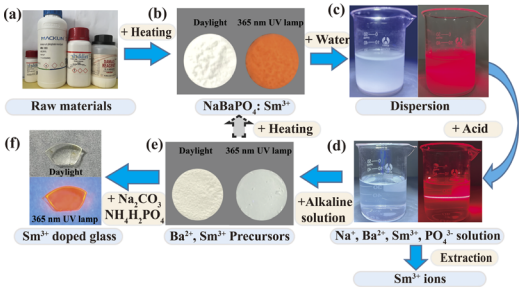

Fig. 1 Recycling process of Sm^{3+} ions from a phosphor to a glass, (a) the raw materials, (b) the $NaBaPO_4$:Sm^{3+} phosphor, (c) the dispersion of the phosphor, (d) the solution after adding acid, (e) the Sm^{3+} and Ba^{2+} containing precipitation and (f) the Sm^{3+} doped glass.

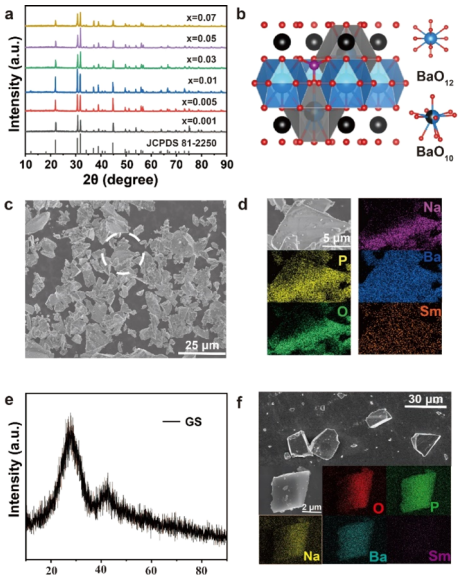

Fig. 2 (a) XRD patterns of $NaBa_{1-x}PO_4$:xSm^{3+} samples. (b) The crystal structure of NBP. (c) SEM image and (d) EDS elemental mapping images. (e) XRD patterns of GS samples. (f) SEM and EDS elemental mapping images of GS samples.

 © 2024 The Author(s). Published by the Royal Society of Chemistry

Open Access Article. Published on 27 March 2024. Downloaded on 12/4/2025 5:26:13 PM.
This article is licensed under a Creative Commons Attribution-NonCommercial 3.0 Unported Licence.

similar ion radii. Since Na has a weak ionization energy, it is easy for it to lose one electron to form Na^+ ion, which has a high polarization. The layer structure was destroyed due to the Na^+ attraction with the oxygen atoms of water molecules with the formation of a more stable system (Na–OH–H). This was why the NBPS partially dissolved in water and formed a homogeneous dispersion. The Sm^{3+} ions in the Na^+ lattice site were then dissociated from the crystal and dissolved into the water, leading to the vanishing of the orange-red emission. After adding a proper amount of phosphoric acid, the Ba–O–P layers were destroyed when the pH reached 2–3, causing the complete dissolution of the NBPS. The particle size of the sample was about 5–10 μm. Energy dispersive spectroscopy (EDS) with element mapping confirmed the presence of the constituent elements of NBPS and the doping of Sm^{3+} in the lattices.

In comparison, the XRD patterns of the GS sample indicated the appearance of the apatite-type structure attributed to $Ba_3(PO_4)_2$. The crystalline size of the structure was about 0.14 nm, which was much smaller than that of NBPS. However, GS was a bulk material (Fig. 1f). Even though grinding was performed, a grain size about 30 μm was still observed (Fig. 2f). Therefore, the major part of GS material was amorphous. Ba, Na, and P–O (Fig. 2b) had a disordered system with some NBPS dissolved in water. Meanwhile, Sm^{3+} was successfully doped into the system, as indicated by elemental EDS mapping.

The fluorescence of the NBPS and GS was investigated to confirm Sm^{3+} doping and its recyclability. As shown in Fig. 3b and S4,† the NBPS showed emission peaks at 565, 600, 645 and 710 nm under 403 nm excitation, corresponding to the $^4G_{5/2}$ to $^6H_{x/2}$ (x = 5, 7, 9 and 11) transitions, which were the feature fluorescence of Sm^{3+} ions.[22–24] Thus, the CIE 1931 chromaticity and correlated color temperature (CCT) were about (0.60, 0.40) and 1627 K, respectively, and the point is correspondent to orange-red emission. The excitation spectrum monitoring the 643 nm emission was in the 340–500 nm excitation range, which matched with the emission range of LED chips, and it also indicated the $^6H_{5/2}$ to $^4K_{17/2}$ (342 nm), $^4H_{7/2}$ (361 nm), $^4P_{7/2}$ (374 nm), $^4F_{7/2}$ (403 nm), $^4I_{15/2}$ (438 nm), and $^4I_{13/2}$ (474 nm) transitions of the Sm^{3+} ions, confirmed by the optical absorption (Fig. S4†). The doping concentrations of Sm^{3+} for the promising fluorescent intensity were 1.0–5.0 mol%, covering the level used for recycling test in the present work.

On the other hand, the GS sample also exhibited the feature excitation and emission spectra of the Sm^{3+} ions. The CIE 1931 chromaticity and CCT were about (0.60, 0.40) and 1627 K respectively, indicating an orange-red emission (Fig. S5 and Table S3†). The fluorescent decay for both NBPS and GS were about 2.0 ms (Fig. S6†), which confirmed the forbidden f–f transition induced in the asymmetric structure or system for the lanthanide series. It further confirmed that Sm^{3+} ions could be successfully recycled from the NBPS and reused for GS. Therefore, a completed cycle for Sm^{3+} from the phosphor and the glass was demonstrated by adjusting the pH to moderate acid and mild alkaline conditions, respectively.

The feature fluorescence of Sm^{3+} in the orange-red area enabled the NBPS potential application in warm white-light LEDs. In addition to the emission color and suitable band gap (Fig. S4†), the thermal stability of NBPS was also promising for the LEDs since about 90% of the fluorescent intensity was preserved at 150 °C (Fig. S7b†). It is dependent on the activation energy for thermal quenching of about 0.17 eV (Fig. S7c†), which was relatively high for phonon transition. Meanwhile, the thermal stability of GS was also considerable. About 75% of the fluorescent intensity was preserved, corresponding to the activation energy of about 0.25 eV (Fig. S7d and f†). Taking advantage of thermal stability, transparency and metastable states of the f–f transition, the GS could be potentially used as an optical glass, especially as the working medium for high-power lasers, and also the optical fibers. The feature emission of Sm^{3+} in both NBPS phosphor and GS could be observed under a 405 nm LED chip excitation (Fig. 4), confirming their expected usages. Therefore, NPBS, GS and Sm^{3+} recycling showed their commercial value for the future urban mining of lanthanides.

In conclusion, the Sm^{3+}-doped NPB phosphors were introduced to confirm the possibility of Sm^{3+} recovery. Due to the solubility of NBP under a moderate acid condition, Sm^{3+} was extractable using a small amount of phosphoric acid, which is less corrosive and hazardous than the sulfuric acid usually used in traditional metallurgy. The product containing the Sm^{3+} compound was collected when the solution was adjusted to a mild alkaline circumstance, and it was reused to synthesize an Sm^{3+}-doped glass successfully. Therefore, a recycling process for Sm^{3+} from a phosphor and its reuse in a glass were demonstrated. Due to the similar chemical properties, other lanthanide elements incorporated in phosphate-based

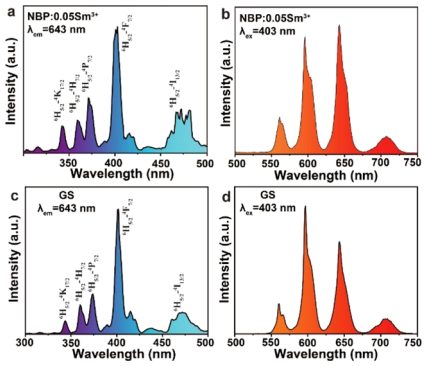

Fig. 3 (a) Excitation spectrum of NBP:0.05Sm^{3+} phosphor (λ_{em} = 643 nm) and (b) PL curves of the NBP:0.05Sm^{3+} powder. (c) Excitation spectrum of GS. (d) PL curves of GS.

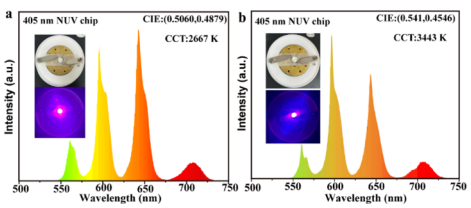

Fig. 4 Electroluminescence spectrum of the fabricated red LED based on a 405 nm chip. (a) NBP:Sm^{3+}. (b) GS samples.

Open Access Article. Published on 27 March 2024. Downloaded on 12/4/2025 5:26:13 PM.
This article is licensed under a Creative Commons Attribution-NonCommercial 3.0 Unported Licence.

materials could be recycled in a similar way. This work provided a successful case study for the urban mining of the lanthanides in a green and sustainable way. Future works can be performed to improve the fluorescence in optical materials, catalytic performance in chemical engineering and electromagnetic properties in the information storage of lanthanides.

Conflicts of interest

The authors declare that they have no known competing financial interests or personal relationships that could have appeared to influence the work reported in this paper.

Notes and references

1 Y.-F. Liu, S.-G. Zhang, B. Liu and H.-L. Shen, *Rare Met.*, 2017, **38**, 299–305.
2 T. G. Ambaye, M. Vaccari, F. D. Castro, S. Prasad and S. Rtimi, *Environ. Sci. Pollut. Res.*, 2020, **27**, 36052–36074.
3 C. V. Ramana, R. S. Vemuri, V. V. Kaichev, V. A. Kochubey, A. A. Saraev and V. V. Atuchin, *ACS Appl. Mater. Interfaces*, 2011, **3**, 4370–4373.
4 V. A. Petrov, G. V. Kuptsov, A. O. Kuptsova, V. V. Atuchin, E. V. Stroganova and V. V. Petrov, *Photonics*, 2023, **10**, 849.
5 A. B. Patil, M. Tarik, R. P. W. J. Struis and C. Ludwig, *Resour., Conserv. Recycl.*, 2021, **164**, 105153.
6 J. Pan, B. V. Hassas, M. Rezaee, C. Zhou and S. V. Pisupati, *J. Cleaner Prod.*, 2021, **284**, 124725.
7 N. Dhawan and H. Tanvar, *Sustainable Mater. Technol.*, 2022, **32**, e00401.
8 B. Mwewa, M. Tadie, S. Ndlovu, G. S. Simate and E. Matinde, *J. Environ. Chem. Eng.*, 2022, **10**, 107704.
9 H. Liu, S. Li, B. Wang, K. Wang, R. Wu, C. Ekberg and A. A. Volinsky, *J. Cleaner Prod.*, 2019, **238**, 117998.
10 Z. Xia, Y. Zhang, M. S. Molokeev and V. V. Atuchin, *J. Phys. Chem. C*, 2013, **117**, 20847–20854.
11 H. Ji, L. Wang, M. S. Molokeev, N. Hirosaki, R. Xie, Z. Huang, Z. Xia, O. M. ten Kate, L. Liu and V. V. Atuchin, *J. Mater. Chem. C*, 2016, **4**, 6855–6863.
12 C.-S. Lim, A. Aleksandrovsky, M. Molokeev, A. Oreshonkov and V. Atuchin, *Molecules*, 2021, **26**, 7357.
13 Z. Hua, A. Geng, Z. Tang, Z. Zhao, H. Liu, Y. Yao and Y. Yang, *J. Environ. Manage.*, 2019, **249**, 109383.
14 D. Avdibegovic and K. Binnemans, *RSC Adv.*, 2021, **11**, 8207–8217.
15 X. Tian, X. Yin, Y. gong, Y. Wu, Z. Tan and P. Xu, *J. Cleaner Prod.*, 2016, **135**, 1210–1217.
16 V. Singh, S. Mahamuda, A. S. Rao, J. L. Rao and M. Irfan, *Optik*, 2020, **206**, 164086.
17 S. Choi, Y. J. Yun, S. J. Kim and H.-K. Jung, *Opt. Lett.*, 2013, **38**, 1346–1348.
18 L. He, Q. Xu, W. Li, Q. Dong and W. Sun, *J. Rare Earths*, 2022, **40**, 338–344.
19 J. Ait Brahim, A. Merroune, H. Mazouz and R. Beniazza, *J. Ind. Eng. Chem.*, 2023, **127**, 446–453.
20 C. H. Yen and R. Cheong, *Minerals*, 2021, **11**, 287.
21 J. Hong, L. Lin, X. Li, J. Xie, Q. Qin and Z. Zheng, *Opt. Mater.*, 2019, **98**, 109471.
22 Y. G. Denisenko, A. E. Sedykh, S. A. Basova, V. V. Atuchin, M. S. Molokeev, A. S. Aleksandrovsky, A. S. Krylov, A. S. Oreshonkov, N. A. Khritokhin, E. I. Sal'nikova, O. V. Andreev and K. Müller-Buschbaum, *Adv. Powder Technol.*, 2021, **32**, 3943–3953.
23 V. V. Atuchin, A. S. Aleksandrovsky, M. S. Molokeev, A. S. Krylov, A. S. Oreshonkov and D. Zhou, *J. Alloys Compd.*, 2017, **729**, 843–849.
24 V. V. Atuchin, A. S. Aleksandrovsky, O. D. Chimitova, C.-P. Diao, T. A. Gavrilova, V. G. Kesler, M. S. Molokeev, A. S. Krylov, B. G. Bazarov, J. G. Bazarova and Z. Lin, *Dalton Trans.*, 2015, **44**, 1805–1815.

 © 2024 The Author(s). Published by the Royal Society of Chemistry